

Probing the Contribution of Vertical Processing Layers of the Retina to White-Noise Electrical Stimulation Responses

Author:

Zha, M; Muralidharan, M; Ly, K; Guo, T; Von Wegner, F; Shabani, H; Hosseinzadeh, Z; Lovell, NH; Rathbun, DL; Shivdasani, MN

Publication details:

Proceedings of the Annual International Conference of the IEEE Engineering in Medicine and Biology Society, EMBS
v. 00
Medium: Print
pp. 1 - 4
9798350324471 (ISBN)
1557-170X (ISSN); 2694-0604 (ISSN)

Event details:

2023 45th Annual International Conference of the IEEE Engineering in Medicine & Biology Society (EMBC)
United States
2023-07-24 - 2023-07-27

Publication Date:

2023-01-01

Publisher DOI:

<https://doi.org/10.1109/EMBC40787.2023.10340816>

License:

<https://creativecommons.org/licenses/by/4.0/>

Link to license to see what you are allowed to do with this resource.

Downloaded from http://hdl.handle.net/1959.4/unsworks_85144 in <https://unsworks.unsw.edu.au> on 2024-04-28

Probing the Contribution of Vertical Processing Layers of the Retina to White-Noise Electrical Stimulation Responses

Mingsong Zha, Madhuvanathi Muralidharan, Keith Ly, *Student Member, IEEE*, Tianruo Guo, *Senior Member, IEEE*, Frederic von Wegner, Hamed Shabani, Zohreh Hosseinzadeh, Nigel H. Lovell, *Fellow, IEEE*, Daniel L. Rathbun and Mohit N. Shivdasani, *Senior Member, IEEE*

Abstract—Optimal stimulus parameters for epiretinal prostheses have been investigated by analyzing retinal ganglion cell (RGC) spiking responses to white-noise electrical stimulation, through a spike-triggered average (STA) analysis technique. However, it is currently unknown as to activation of which retinal cells contribute to features of the STA. We conducted whole-cell patch clamping recordings in ON and OFF RGCs in response to white-noise epiretinal electrical stimulation by using different inhibitors of synaptic transmission in a healthy retina. An mGluR6 agonist, L-AP4, was firstly used to selectively block the output of photoreceptors (PRs) to ON bipolar cells (BCs). We subsequently fully blocked all synaptic inputs to RGCs using a combination of pharmacological agents. Our data shows that PRs dominate the ability of ON RGCs to integrate electrical pulses and form a unique STA shape, while BCs do not contribute in any way. In addition, our results demonstrate that the ability of OFF RGCs to integrate pulses is consistently impaired after blocking the PR to ON BC pathway. We hypothesize that the mechanisms underlying this co-effect are related to the narrow field AII amacrine cells connecting ON and OFF pathways.

Clinical Relevance—Recent retinal studies recorded mirror-inverted STAs in ON and OFF retinal pathways, thus raising the possibility of designing a stimulation approach that can differentially activate ON and OFF pathways with electrical stimulation. However, the detailed contribution of three major retinal cell layers in forming characteristic STAs is still unclear. It is of great clinical relevance to investigate the isolated contribution of PRs to the electrically driven STA since PRs progressively degenerate in the course of retinal disease.

I. INTRODUCTION

Recent retinal electrical stimulation studies have attempted to characterize the preferred time-varying stimuli to activate functionally distinct retinal pathways using a spike-triggered average (STA) technique applied to responses of retinal ganglion cells (RGCs) to white-noise stimulation (WNS). A particular finding from these studies has been the ability to generate mirror-inverted electrical STA (eSTA) shapes in ON and OFF RGCs [1-3]. These discoveries have raised hopes to design a network-driven stimulation approach enabling differential targeting of the ON and OFF pathways, currently unachievable with conventional stimulation

approaches. However, the isolated contribution of various retinal network cell types such as photoreceptors (PRs), bipolar cells (BCs) in forming ON and OFF mirror-inverted eSTAs is unclear [1, 2]. Mirror-inverted eSTAs have also been identified in the degenerated retina [3-5], providing some evidence that BCs play a role in forming mirror-inverted eSTA shapes in the absence of PRs.

This study aimed to determine changes in the eSTA shape in ON and OFF RGCs obtained from WNS, as a result of blocking different transmission pathways using two groups of pharmacological blockers and whole-cell patch-clamping recordings in a healthy retina. We hypothesized that both PRs and BCs should have the ability to integrate WNS thus contributing to the overall eSTA.

II. METHODS

A. Ex Vivo Whole-Cell Patch Clamping in Mice Retina

All procedures performed in this study were approved by the UNSW Animal Care and Ethics committee. C57BL/6J mice (post-natal day P28–P56, Australian BioResource, Mossvale, NSW, Australia) were dark-adapted for at least half a day before each experiment. Immediately post-euthanasia, the retina was extracted and dissected into pieces for patch clamping. Retinal pieces were initially mounted, ganglion-cell side up, on a modified Millicell Biopore membrane filter insert (PICM01250, Millipore, Billerica, MA, USA). The membrane insert was placed in an imaging chamber (RC-40HP, Warner Instruments, Hamden, CT, USA) and held in place by petroleum jelly (Vaseline). The imaging chamber was heated to approximately 33°–35°C, perfused with extracellular solution at a rate of 3–4 mL/min, and maintained at pH 7.4. All procedures were conducted in a room dimly illuminated with red light.

Whole-cell patch clamping as described in our previous *ex vivo* studies [6-8] was conducted. In brief, we used glass pipettes (Warner Instruments, Hamden, CT, USA) with tip resistances of 3 – 6 M Ω . All cell responses were acquired using the Multiclamp 700B amplifier (Molecular Devices, Sunnyvale, CA, USA), low-pass filtered at 10 kHz, sampled at 50 kHz using the Digidata 1440A acquisition system, and displayed using the corresponding pCLAMP 10 software

* This study was supported by the Australia–Germany Joint Research Cooperation Scheme (#RG181337) to M. Shivdasani and Deutsche Forschungsgemeinschaft (HO 6221/1-1) to Z. Hosseinzadeh.

M. Zha, M. Muralidharan, K. Ly, T. Guo, N.H. Lovell and M. N. Shivdasani are with the Graduate School of Biomedical Engineering and Tyree Institute of Health Engineering, UNSW Sydney, NSW 2052, Australia. F. von Wegner is with the School of Biomedical Sciences, UNSW Sydney,

H. Shabani is with Systems Neuroscience Center, School of Medicine, University of Pittsburgh, Pittsburgh, PA, USA. Z. Hosseinzadeh is with Paul Flechsig Institute of Brain Research, University of Leipzig, Leipzig, Germany. D. L. Rathbun is with Department of Ophthalmology, Henry Ford Health System, Detroit, MI 48202, USA.
E-mail for correspondence: m.shivdasani@unsw.edu.au

(Molecular Devices, Sunnyvale, CA, USA). ON and OFF RGCs were identified by illuminating the retina with directed full-field white light flashes.

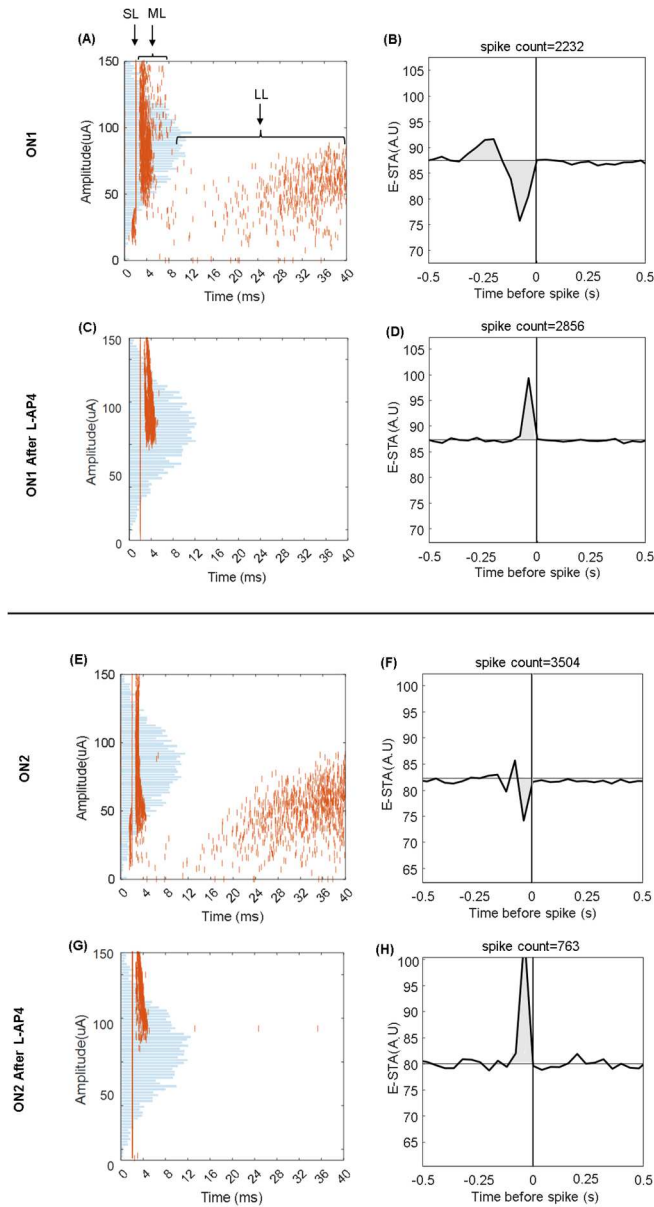


Figure 1. Spike raster (left) and eSTA (right) plots before and after L-AP4 application from two ON RGCs. The blue histogram in panels A, C, E and G represent the distribution of the WN pulse amplitudes. Recorded RGC spikes are represented by short vertical orange lines. The grey areas in panels B, D, F and H represent the eSTA, calculated by averaging the 25 WNS pulse amplitudes (corresponding to a 1s stimulus snippet) before each network-mediated spike (ML and LL spikes only). AU: arbitrary unit, SL: short latency, ML: middle latency, LL: long latency.

B. White-Noise Stimulation and Electrical Spike-triggered Average

A 25- μm diameter platinum-iridium stimulating electrode was placed 40 μm above the patched RGC soma [9]. A platinum return electrode was placed approximately 2 cm distant from the tissue in the bath to enable a monopolar configuration. Cathodic-first biphasic charge-balanced constant current pulses with 1 ms phase duration and no inter-

phase delay were used. Amplitudes for WNS were drawn from a Gaussian distribution and pulses were presented at 25 Hz [1, 5]. We set the mean stimulation amplitude for each RGC relative to a threshold current obtained using single pulse stimulation and set the standard deviation to 30 μA for all sequences. The upper limit was set to 200 μA to minimize the risk of tissue damage. Taking advantage of high-resolution single-cell patch clamp recordings, we reduced the WNS duration from 1 hour to 2.5 mins without influencing the observed eSTA quality.

The eSTA was calculated by averaging 25 WNS pulse amplitudes (corresponding to a 1 s stimulus snippet) before each network-mediated spike [10]. Spikes driven by direct RGC activation (within 2 ms post-stimulus) were excluded. STA deflections that were significantly above or below the WNS mean for positive and negative deflections were further analyzed. For each deflection, we extracted two features: (1) Deflection width, defined as the period from the first point crossing the mean amplitude to the next zero crossing period (a longer deflection indicated that retinal cells contributing to the eSTA could integrate multiple pulses). Based on a 25 Hz stimulation rate, a deflection width less than 100 ms indicated that no integration of multiple pulses occurred over 1 s of stimulation and instead responses were evoked by individual pulses instead. (2) Deflection peak latency, defined by the time from the maximum point in a positive deflection or the minimum point in a negative deflection to the time of the spike (0 ms in the eSTA).

C. Pharmacological Blockers

Following baseline eSTA recordings in healthy retina, an mGluR6 agonist, L-AP4 (0.02 mM), was first used to block PR to ON BC synaptic transmission. After that, we applied the following combination of drugs to fully block synaptic inputs to RGCs [6, 11, 12]: (1) strychnine (0.01 mM) to block glycinergic receptors, (2) picrotoxin (0.1 mM) to block GABA receptors, (3) NBQX (0.01 mM, 2,3-dihydroxy-6-nitro-7-sulfamoyl-benzoquinoline) to block AMPA/Kainate receptors, (4) D-AP5 (0.05 mM, (2R)-amino-5-phosphonovaleric acid) to block NMDA receptors and (5) L-AP4 (0.02 mM) to agonist mGluR6 receptors. Successful L-AP4 blocking of the ON pathway was determined by the absence of light-elicited ON RGC spikes, which was observed around 5 mins post application. For the OFF pathway, the effect of L-AP4 could not be directly observed, so we waited for 5 mins post application [6] before we started the following electrical stimulation procedure. In total, we recorded eSTA responses in 2 ON RGCs and 3 OFF RGCs pre- and post-L-AP4. 2 OFF RGCs were further blocked by full pharmacological blockade.

III. RESULTS AND DISCUSSION

A. RGCs responses prior to blockers

Raster plots of RGC spikes showed three distinct spike clusters (Figure 1); short latency (SL): spikes recorded within 2 ms post stimulus, middle latency (ML): latency between 2-8 ms post stimulus and long latency (LL): latency >8 ms. ML and LL spike latencies exhibited large variability, particularly in the low stimulation amplitude range.

Prior to application of synaptic blockers, ON and OFF RGCs showed similar patterns of SL and ML spikes but different patterns of LL spikes. In particular, LL spikes were primarily observed at relatively lower amplitudes in ON RGCs (Fig. 1A, E), but at higher amplitudes in OFF RGCs (Fig. 2A, G). In addition, LL spikes in OFF RGCs had relatively shorter latencies than those evoked in ON RGCs.

As shown in Fig. 1B and F, eSTAs in ON RGCs prior to blockers demonstrated a positive deflection (second deflection) followed by a negative deflection (first deflection), indicating that they fired most strongly to low amplitude pulses followed by high amplitude pulses. Conversely, as shown in Fig. 2B and H, OFF RGCs exhibited an opposite pattern with a negative first deflection and positive second deflection. These STA patterns closely agreed with published eSTAs in ON and OFF RGCs [2, 5]. In addition, ON and OFF eSTAs showed characteristic deflection widths as reported by previous studies [1, 2, 5]. ON RGCs showed higher first deflection width and latency, while OFF RGCs showed higher second deflection width and latency.

B. The Effect of L-AP4 on ON and OFF eSTAs

As shown in Fig. 1D and H, eSTAs for the two ON RGCs recorded became almost identical after application of L-AP4. Post L-AP4 both ON eSTAs demonstrated a single monophasic positive deflection, indicating that the retina did not integrate multiple pulses. We also observed (Fig. 1C and G) that all electrically elicited ML and LL spikes at low stimulation amplitudes were abolished, however ML spikes were still evoked, suggesting that LL spikes were evoked as a result of activation of PRs and ML spikes as a result of activation of BCs.

In contrast, OFF eSTAs (Fig. 2D and J) only underwent minor changes post L-AP4. There were two trends observed: (1) the peak latency of the first deflection remained unchanged. (2) The peak latency of the second deflection showed a significant decrease. In addition, post L-AP4 OFF RGCs showed altered LL spiking patterns but not ML spiking.

D. The Effect of Full Pharmacological Blockade on OFF eSTAs

We were unfortunately not able to assess the effects of full blockers on ON cells. Interestingly, OFF RGCs demonstrated a variable response after the full pharmacological blockade. For example, the OFF RGC shown in Fig. 2E displayed totally abolished ML and LL spikes post full blocker. Therefore, no eSTA could be calculated for this cell. In contrast, another OFF RGC (Fig. 2O) exhibited no ML spikes in control and L-AP4 conditions. However, the same cell demonstrated strong ML spikes elicited between 50 and 150 μ A after the application of full blocker. At the same time, many LL spikes survived at higher stimulation amplitudes (80-150 μ A) despite reduction in overall spike counts. OFF eSTAs demonstrated a monophasic positive deflection, indicating that the retina did not integrate multiple pulses.

IV. DISCUSSION AND CONCLUSION

A. The effect of L-AP4 on the ON pathway

The two ON eSTAs after L-AP4 application demonstrated

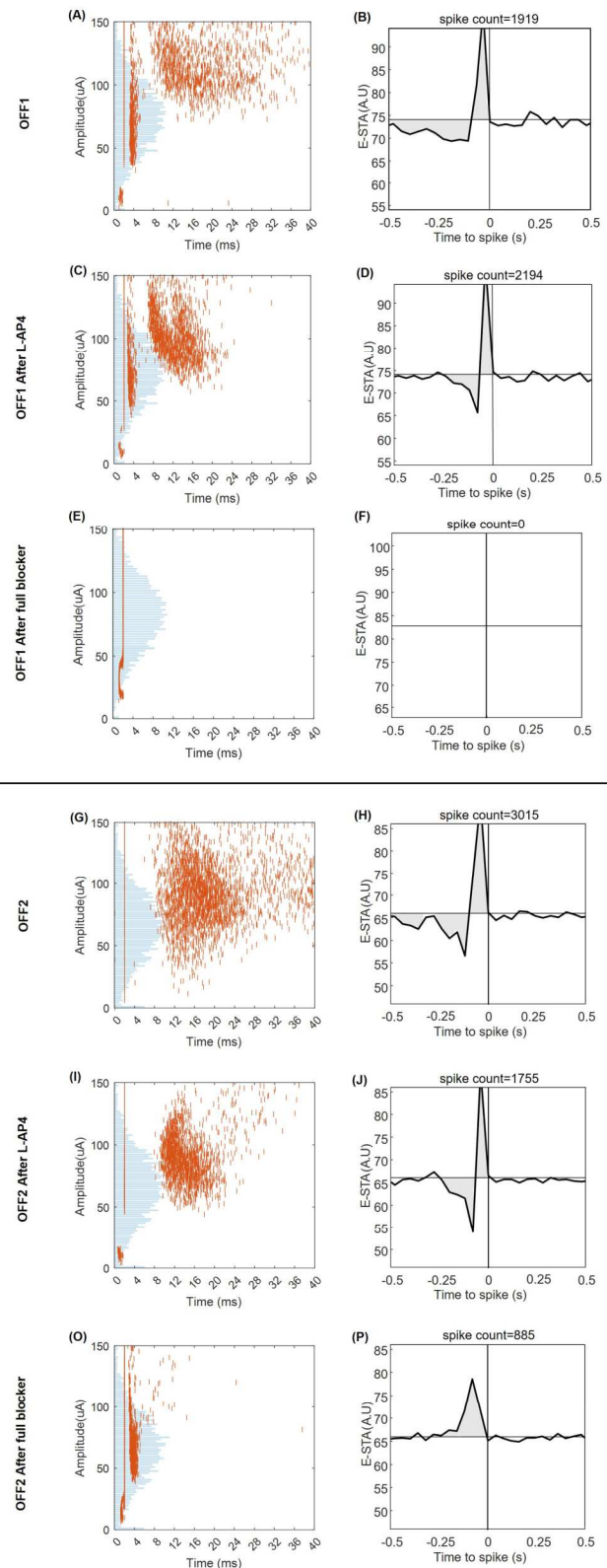


Figure 2. Spike raster plots and eSTA shapes before (panel A, G), after L-AP4 (panels C, I) and after full blocker (E, O) in two OFF RGCs. A third OFF RGC recorded without the application of full blocker is not shown.

single monophasic positive deflections, indicating that ON BCs alone are not capable of integrating consecutive pulses. In addition, reversal of the first deflection polarity after L-AP4 suggests the mirror-inverted eSTAs observed between

the ON and OFF pathways prior to blocker application was mostly driven by PRs.

Previous studies suggested that eSTAs observed in degenerated retina are driven by LL spikes and are usually biphasic and triphasic [3-5]. These data suggested that the remodeled retinal network's ability to integrate pulses was impaired. Our study provides further evidence that the mirror inverted STAs identified in degenerated retina in previous studies likely arose from contribution of surviving PRs rather than BCs. However, the exact contribution of other inner retinal neurons in shaping the eSTA is still an open question.

Our data showed that the OFF pathway was also influenced by pharmacologically blocking the PR-ON BC connection. First, a significant reduction in LL spike count was observed post-L-AP4 application. Second, a significantly increased threshold for network-mediated spikes was identified. One hypothesis is that L-AP4-induced ON BC depolarization caused the electrically coupled AII amacrine cells (AII ACs) to send more glycinergic inhibition to OFF BCs and RGCs. These observations indicate a possible important role of AII ACs in forming eSTA. AII ACs electrically couple the ON pathway while sending glycinergic inhibitory input to OFF BCs and RGCs [13, 14]. Additionally, AII ACs do not undergo significant degeneration until later stages of inner retinal remodeling [15]. Therefore, blocking PRs and ON BCs might indirectly influence the integrating ability of OFF pathways by "shifting" the baseline potential of OFF BCs and RGCs. It should be noted that not all OFF pathways are rectified by the ON pathway through AII ACs. In fact, narrow-field AII ACs (the cell "bridging" the ON and OFF pathways) constitute only 10-15% of the total AC population [16], indicating that a subpopulation of OFF BCs and RGCs cannot be influenced by L-AP4. Since there are no selective pharmacological blockers for glutamatergic transmission from PRs to the OFF BC without affecting the rest of the retinal network, investigating the contribution of PRs on OFF eSTAs could be more difficult with *ex vivo* electrophysiology. Computational modelling of retinal network [14, 17, 18] and functionally-distinct RGC activity [19, 20] would be useful in the future to probe the detailed contribution of individual retinal neuron types in forming eSTA.

B. The Effect of Full Pharmacological Blockade on OFF Pathway

The observation that a new cluster of ML spikes appeared in an OFF RGC (Fig 20) after full pharmacological blockade indicates the phenomenon of "dis-inhibition" reported in other studies [21]. Dis-inhibition happens when the full blockade abolished the inhibition that AII ACs exert on OFF BC and RGCs, while failing to block other excitatory input to RGCs, causing a new cluster of spikes to appear on the raster plot. We speculate that the ML and LL spikes post full blockade are more likely to be due to an incomplete blockade.

In summary, our findings support the hypothesis that the mirror-inverted eSTA mostly comes from PR-mediated activation since there was no visible amplitude-dependent difference on ML and SL spikes in ON and OFF RGCs raster plots.

REFERENCES

- [1] S. Sekhar, A. Jalligampala, E. Zrenner, and D. L. Rathbun, "Tickling the retina: integration of subthreshold electrical pulses can activate retinal neurons," *J Neural Eng*, vol. 13, no. 4, p 046004, 2016
- [2] S. Sekhar, A. Jalligampala, E. Zrenner, and D. L. Rathbun, "Correspondence between visual and electrical input filters of ON and OFF mouse retinal ganglion cells," *J Neural Eng*, vol. 14, no. 4, p 046017, 2017
- [3] E. Ho, A. Shmakov, and D. Palanker, "Decoding network-mediated retinal response to electrical stimulation: implications for fidelity of prosthetic vision," *J Neural Eng*, 2020
- [4] D. L. Rathbun, N. Ghorbani, H. Shabani, E. Zrenner, and Z. Hosseinzadeh, "Spike-triggered average electrical stimuli as input filters for bionic vision—a perspective," *J Neural Eng*, vol. 15, no. 6, 2018
- [5] E. Ho, H. Lorach, G. Goetz, F. Laszlo, X. Lei *et al.*, "Temporal structure in spiking patterns of ganglion cells defines perceptual thresholds in rodents with subretinal prosthesis," *Sci Rep*, vol. 8, 2018
- [6] M. Muralidharan, T. Guo, M. N. Shivdasani, D. Tsai, S. Fried *et al.*, "Neural activity of functionally different retinal ganglion cells can be robustly modulated by high-rate electrical pulse trains," *J Neural Eng*, vol. 17, no. 4, p 045013, 2020
- [7] T. Guo, D. Tsai, J. W. Morley, G. J. Suaning, T. Kameneva *et al.*, "Electrical activity of ON and OFF retinal ganglion cells: a modelling study," *J Neural Eng*, vol. 13, no. 2, p 025005, 2016
- [8] T. Guo, D. Tsai, C. Y. Yang, A. Al Abed, P. Twyford *et al.*, "Mediating retinal ganglion cell spike rates using high-frequency electrical stimulation," *Front Neurosci*, vol. 13, p 413, 2019
- [9] T. Guo, C. Y. Yang, D. Tsai, M. Muralidharan, G. J. Suaning *et al.*, "Closed-loop efficient searching of optimal electrical stimulation parameters for preferential excitation of retinal ganglion cells," *Front Neurosci*, vol. 12, p 168, 2018
- [10] E. J. Chichilnisky, "A simple white noise analysis of neuronal light responses," *Network: Comput. Neural Syst.*, vol. 12, no. 2, pp. 199-213, 2001
- [11] Z. Y. Liang and M. A. Freed, "The ON pathway rectifies the OFF pathway of the mammalian retina," *J Neurosci*, vol. 30, no. 16, pp. 5533-5543, 2010
- [12] C. Y. Yang, D. Tsai, T. Guo, S. Dokos, G. J. Suaning *et al.*, "Differential electrical responses in retinal ganglion cell subtypes: effects of synaptic blockade and stimulating electrode location," *J Neural Eng*, vol. 15, no. 4, p 046020, 2018
- [13] D. Raz-Prag, G. Beit-Yaakov, and Y. Hanein, "Electrical stimulation of different retinal components and the effect of asymmetric pulses," *J Neurosci Methods*, vol. 291, pp. 20-27, 2017
- [14] K. Ly, T. Guo, D. Tsai, M. Muralidharan, M. N. Shivdasani *et al.*, "Simulating the impact of photoreceptor loss and inner retinal network changes on electrical activity of the retina," *J Neural Eng*, vol. 19, no. 6, 2022
- [15] B. W. Jones and R. E. Marc, "Retinal remodeling during retinal degeneration," *Exp Eye Res*, vol. 81, no. 2, pp. 123-37, 2005
- [16] U. Grunert and P. R. Martin, "Cell types and cell circuits in human and non-human primate retina," *Prog Retin Eye Res*, p 100844, 2020
- [17] T. Guo, D. Tsai, S. Bai, J. W. Morley, G. J. Suaning *et al.*, "Understanding the retina: a review of computational models of the retina from the single cell to the network level," *Crit Rev Biomed Eng*, vol. 42, no. 5, pp. 419-36, 2014
- [18] S. Dokos and T. Guo, "Computational models of neural retina," in *Encyclopedia of Computational Neuroscience.*, D. Jaeger and R. Jung, Eds. New York:Springer, 2020
- [19] M. L. Italiano, T. R. Guo, N. H. Lovell, and D. Tsai, "Improving the spatial resolution of artificial vision using midretinal ganglion cell populations modeled at the human fovea," *Journal of Neural Engineering*, vol. 19, no. 3, 2022
- [20] X. Y. Song, S. R. Qiu, M. N. Shivdasani, F. Zhou, Z. Y. Liu *et al.*, "An in-silico analysis of electrically evoked responses of midretinal and parasol retinal ganglion cells in different retinal regions," *Journal of Neural Engineering*, vol. 19, no. 2, 2022
- [21] J. Menzler, L. Channappa, and G. Zeck, "Rhythmic ganglion cell activity in bleached and blind adult mouse retinas," *PLoS One*, vol. 9, no. 8, p e106047, 2014